Three-Dimensional Fluid Flow Model for Gas-Stirred Ladles

S.-M. Pan, Y.-H. Ho, and W.-S. Hwang

A three-dimensional mathematical model has been developed to simulate the fluid flow phenomena in gas-stirred ladles. It can predict the velocity profile and flow pattern of the liquid and the gas bubbles. The two-phase fluid flow phenomena were analyzed by using the SOLA-SURF technique supplemented with the K-ε two-equation turbulence model. The interactions between the gas bubble motion and the liquid flow were also considered. The movements of the gas bubbles were calculated and the extent of the plume zone determined. The effects of various design/operation conditions, such as gas flow rate, location of the porous plug, and addition of an immersion hood, can be evaluated. Flow intensity and stirring ability increase with increased gas flow rate. The dead zone near the bottom corner of the ladle exists whether the porous plug is centered or off-centered; this problem only slightly improves when gas flow rate is increased. Addition of an immersion hood not only provides a slag-free and protective atmosphere inside the hood, but also reduces the dead zone.

Keywords

gas-stirred ladle, ladle metallurgy, three-dimensional fluid flow model, two-phase flow

1. Introduction

TO IMPROVE steel quality and simplify operation, the steelmaking process is divided into two stages (Ref 1): (1) primary steelmaking in a furnace to produce raw steel and (2) secondary steelmaking in a ladle with various refining treatments. In recent years gas stirring, a treatment accomplished by blowing argon gas through a porous plug, has been used in the refining ladle for the purposes of desulfurization, degassing, minor composition adjustment, temperature homogenization, and inclusion removal. A schematic diagram of a gas-stirred ladle is shown in Fig. 1. As the gas bubbles are introduced through the porous plug into the ladle, they rise through the melt and cause it to flow. Because of the melt flow, the additives, either desulfurization agents or alloying elements, can be mixed more effectively with the melt. Also, degassing and temperature homogenization can be achieved more readily.

S.-M. Pan, Y.-H. Ho, and **W.-S. Hwang,** Department of Materials Science and Engineering, National Cheng Kung University, Tainan, Taiwan, R.O.C.

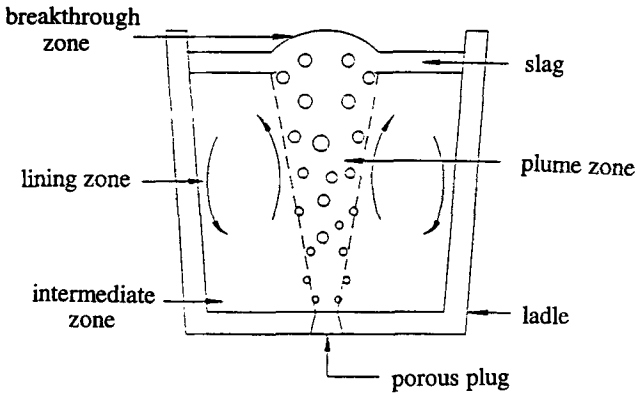

Fig. 1 Schematic diagram of a gas-stirred ladle

However, gas stirring also causes several possible problems, including reoxidation of the molten steel, slag entrapment, and nitrogen pickup. To improve the treatment, a SAC (slag and atmosphere control) process which places an immersion hood in the ladle was suggested (Ref 2). This process is represented schematically in Fig. 2. The basic idea comes from the CAS (composition adjustment system) process pioneered by researchers at Nippon Steel Corporation (Ref 3). When an immersion hood is used, there will be good slag and atmosphere control inside the hood. However, the main concern is the effect of the immersion hood on the turbulent mixing and agitation in the gas-stirred ladle.

Symbols

C_d	drag factor
D	diffusivity
D_e	effective diffusivity
D_b	bubble diameter
F_x, F_y, F_z	drag force by bubbles in the x, y, z direction, respectively
g	gravity
H	height of free surface
K	turbulence kinetic energy
N	total number of bubbles in a unit cell
P	pressure
Q	gas flow rate
R_e	Reynolds number
$\mathbf{U, V, W}$	velocity vector of the liquid in the x, y, z direction, respectively
$\mathbf{U_b, V_b, W_b}$	velocity vector of the bubble in the x, y, z direction, respectively
α_l	void fraction of fluid
α_m	void fraction of a bubble in a unit cell
ε	dissipation rate of turbulence energy
ρ_g	density of gas
ρ_l	density of liquid
ν_e	effective kinematic viscosity
μ_l	viscosity of liquid
ν_m	molecular kinematic viscosity
ν_t	turbulence kinematic viscosity

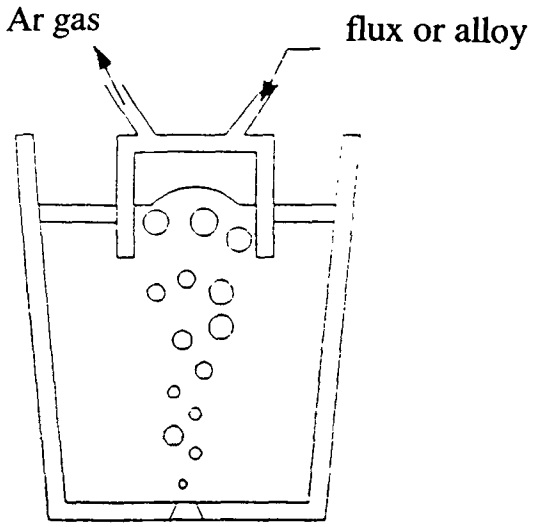

Fig. 2 Schematic diagram of a gas-stirred ladle incorporating the SAC process

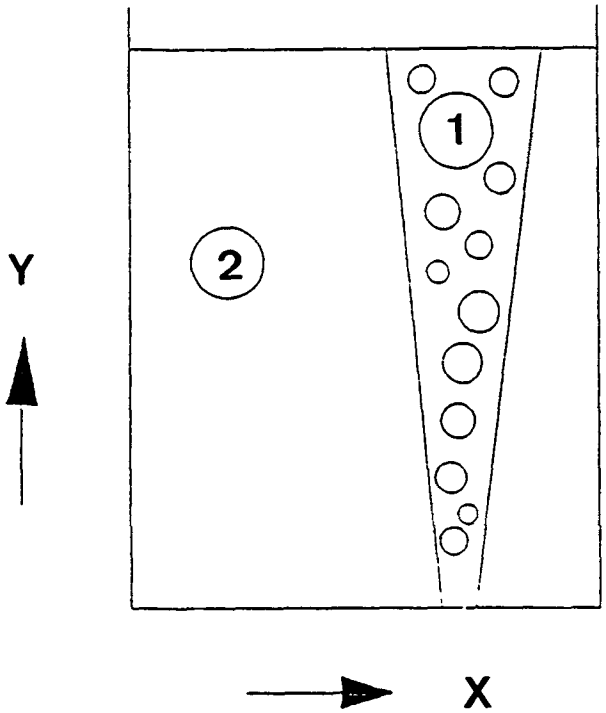

Fig. 3 Schematic diagram of the physical system considered in the mathematical model. (1) Plume zone. (2) Liquid phase zone

In a steelmaking operation, any equipment additions mean significant capital investment and possible operation difficulties. Therefore, to evaluate the feasibility of the SAC process and to design the immersion hood if the process proves beneficial (even with its additional cost and operation difficulties), the interactive flow phenomena of molten steel and gas bubbles under various operating conditions with and without the addition of an immersion hood must be understood.

In the literature, a number of investigations have been carried out with mathematical and/or water models to understand the characteristics of fluid flow and mass transfer phenomena in gas-stirred vessels. However, in most of the mathematical models the extent of the two-phase region and its corresponding void fraction distribution were predetermined by measurements or assumptions. Also, the free surface was assumed to be flat. These assumptions make the mathematical models inadequate for studying the SAC process.

A two-dimensional (2-D) mathematical model of the cylindrical coordinate system (Ref 4) was developed by the authors to simulate the flow phenomena for gas stirring of liquid in a ladle. This model can determine the extent of the two-phase region and calculate the void fraction, allowing the top surface of the liquid to fluctuate. The flow characteristics of interest include flow pattern, velocity profile, surface fluctuation, and bubble dispersion under various operating conditions with and without an immersion hood. The model is capable of handling those cases where the porous plug is located at the center of the ladle bottom. However, it cannot treat problems that arise where the porous plug is located off-center, which is more common in industrial practices.

The purpose of the present study was to develop a three-dimensional (3-D) mathematical model to simulate the flow phenomena for gas stirring of liquid in a ladle regardless of the location of the porous plug.

2. Mathematical Model

2.1 *Description of the Physical Phenomena, with Assumptions and Simplifications for the Mathematical Model*

The gas-stirred ladle is essentially a bubble-driven recirculating flow system. Analysis of the phenomena is a fairly complex fluid mechanics problem. When argon gas is released from the porous plug, it forms gas bubbles of various sizes. Owing to the density difference, the bubbles will float to the top. When the bubbles float, they induce the molten metal to flow; in turn, the flowing melt affects the rising patterns of the bubbles. Observations from the water models show that the two-phase regions are plume shaped. Therefore, the analytical system can be divided into two zones: the plume zone and the liquid phase zone. A schematic diagram of the system is shown in Fig. 3.

To reduce the complexity of the mathematical model, a number of simplifications and assumptions were made:

- The side wall of the ladle is perpendicular to the bottom wall.
- The physical properties of the fluids are constant.
- The bubble size remains constant during flotation.

2.2 *Governing Equations*

It would have been natural to base the 3-D model on the previous 2-D model with cylindrical coordinates. However, the cylindrical coordinate system made it difficult to appropriately treat the off-centered porous plug and the central region of the ladle. Therefore, the 3-D model was developed in the Cartesian coordinate system.

2.2.1 Flow Equation for Liquid Phase

The flow equations for the liquid in the 3-D Cartesian coordinate system can be represented as:

Continuity equation

$$\frac{\partial \alpha_l}{\partial t}+\frac{\partial \alpha_l U}{\partial x}+\frac{\partial \alpha_l V}{\partial y}+\frac{\partial \alpha_l W}{\partial z}=0 \qquad \text{(Eq 1)}$$

Momentum equation

$$\frac{\partial \alpha_l U}{\partial t}+U\frac{\partial \alpha_l U}{\partial x}+V\frac{\partial \alpha_l U}{\partial y}+W\frac{\partial \alpha_l U}{\partial z}=-\frac{\alpha_l}{\rho_l}\frac{\partial P}{\partial x}+F_x+\frac{\partial}{\partial x}\left[\alpha_l \nu_e\left(\frac{\partial U}{\partial x}+\frac{\partial U}{\partial x}\right)\right]+\frac{\partial}{\partial y}\left[\alpha_l \nu_e\left(\frac{\partial U}{\partial y}+\frac{\partial V}{\partial x}\right)\right]+\frac{\partial}{\partial z}\left[\alpha_l \nu_e\left(\frac{\partial U}{\partial z}+\frac{\partial W}{\partial x}\right)\right] \qquad \text{(Eq 2)}$$

$$\frac{\partial \alpha_l V}{\partial t}+U\frac{\partial \alpha_l V}{\partial x}+V\frac{\partial \alpha_l V}{\partial y}+W\frac{\partial \alpha_l V}{\partial z}=-\frac{\alpha_l}{\rho_l}\frac{\partial P}{\partial y}+F_y+\frac{\partial}{\partial x}\left[\alpha_l \nu_e\left(\frac{\partial V}{\partial x}+\frac{\partial U}{\partial y}\right)\right]+\frac{\partial}{\partial y}\left[\alpha_l \nu_e\left(\frac{\partial V}{\partial y}+\frac{\partial V}{\partial y}\right)\right]+\frac{\partial}{\partial z}\left[\alpha_l \nu_e\left(\frac{\partial V}{\partial z}+\frac{\partial W}{\partial y}\right)\right]+\alpha_l g \qquad \text{(Eq 3)}$$

$$\frac{\partial \alpha_l W}{\partial t}+U\frac{\partial \alpha_l W}{\partial x}+V\frac{\partial \alpha_l W}{\partial y}+W\frac{\partial \alpha_l W}{\partial z}=-\frac{\alpha_l}{\rho_l}\frac{\partial P}{\partial z}+F_z+\frac{\partial}{\partial x}\left[\alpha_l \nu_e\left(\frac{\partial W}{\partial x}+\frac{\partial U}{\partial z}\right)\right]+\frac{\partial}{\partial y}\left[\alpha_l \nu_e\left(\frac{\partial W}{\partial y}+\frac{\partial V}{\partial z}\right)\right]+\frac{\partial}{\partial z}\left[\alpha_l \nu_e\left(\frac{\partial W}{\partial z}+\frac{\partial W}{\partial z}\right)\right] \qquad \text{(Eq 4)}$$

where

$$F_x=\sum_{m=1}^{N}\frac{3}{4}\frac{\mu_l}{D_b^2}C_d R_e\left(U_b-U\right)\alpha_m \qquad \text{(Eq 5)}$$

$$F_y=\sum_{m=1}^{N}\frac{3}{4}\frac{\mu_l}{D_b^2}C_d R_e\left(V_b-V\right)\alpha_m \qquad \text{(Eq 6)}$$

$$F_z=\sum_{m=1}^{N}\frac{3}{4}\frac{\mu_l}{D_b^2}C_d R_e\left(W_b-W\right)\alpha_m \qquad \text{(Eq 7)}$$

2.2.2 Flow Equations for Gas Bubble

The equations of motion for the gas bubble rising in the liquid can be represented as:

$$\frac{dU_b}{dt}=-\frac{3}{4}\frac{\mu_l}{\rho_l D_b^2}C_d R_e\left(U_b-U\right)+\frac{\rho_l}{\rho_g}\frac{dU}{dt}-\frac{1}{2}\frac{\rho_l}{\rho_g}\left(\frac{dU_b}{dt}-\frac{dU}{dt}\right) \qquad \text{(Eq 8)}$$

$$\frac{dV_b}{dt}=-\frac{3}{4}\frac{\mu_l}{\rho_l D_b^2}C_d R_e\left(V_b-V\right)+\frac{\rho_l}{\rho_g}\frac{dV}{dt}-\frac{1}{2}\frac{\rho_l}{\rho_g}\left(\frac{dV_b}{dt}-\frac{dV}{dt}\right)+\left(1-\frac{\rho_l}{\rho_g}\right)g \qquad \text{(Eq 9)}$$

$$\frac{dW_b}{dt}=-\frac{3}{4}\frac{\mu_l}{\rho_l D_b^2}C_d R_e\left(W_b-W\right)+\frac{\rho_l}{\rho_g}\frac{dW}{dt}-\frac{1}{2}\frac{\rho_l}{\rho_g}\left(\frac{dW_b}{dt}-\frac{dW}{dt}\right) \qquad \text{(Eq 10)}$$

where

$$R_e=\frac{\rho_l D_b |V_r|}{\mu_l} \qquad \text{(Eq 11)}$$

$$C_d=\frac{24}{R_e}\left[1+0.15R_e^{0.687}+\frac{0.42}{1+(4.25\times 10^4/R_e^{1.16})}\right] \qquad \text{(Eq 12)}$$

When the size and frequency of the bubbles released from the plug are known, the velocity of each bubble can be calculated from Eq 8 to 10. Subsequently, the positions of each bubble, the void fraction of each control volume, and the bubble pathlines can be obtained. The bubble size and release frequency depend mainly on the gas flow rate, plug diameter, and physical properties of the fluids. For gas stirring, Davidson and Schüler (Ref 5), neglecting surface tension and viscosity effects and considering only the balance between inertia force and buoyancy force, derived a formula to approximate the bubble size at high gas flow rate:

$$D_b=0.35\left(\frac{Q^2}{g}\right)^{0.2} \qquad \text{(Eq 13)}$$

With the bubble size known, the release frequency can be calculated from the gas flow rate used.

2.2.3 Governing Equations for the Turbulence Model

The turbulence model used in this study is the K-ε two-equation model (Ref 6). The governing equations for this model are of these forms:

Turbulence kinetic energy, K

$$\frac{\partial \alpha_l K}{\partial t} + U\frac{\partial \alpha_l K}{\partial x} + V\frac{\partial \alpha_l K}{\partial y} + W\frac{\partial \alpha_l K}{\partial z} = \frac{\partial}{\partial x}\left(\alpha_l \frac{\nu_t}{\sigma_k}\frac{\partial K}{\partial x}\right) + \frac{\partial}{\partial y}\left(\alpha_l \frac{\nu_t}{\sigma_k}\frac{\partial K}{\partial y}\right) + \frac{\partial}{\partial z}\left(\alpha_l \frac{\nu_t}{\sigma_k}\frac{\partial K}{\partial z}\right) - \alpha_l \varepsilon + \alpha_l \nu_t \left[2\left(\frac{\partial U}{\partial x}\right)^2 + 2\left(\frac{\partial V}{\partial y}\right)^2 + 2\left(\frac{\partial W}{\partial z}\right)^2 + \left(\frac{\partial U}{\partial y} + \frac{\partial V}{\partial x}\right)^2 + \left(\frac{\partial U}{\partial z} + \frac{\partial W}{\partial x}\right)^2 + \left(\frac{\partial V}{\partial z} + \frac{\partial W}{\partial y}\right)^2 \right] \quad \text{(Eq 14)}$$

Dissipation rate of turbulence kinetic energy, ε

$$\frac{\partial \alpha_l \varepsilon}{\partial t} + U\frac{\partial \alpha_l \varepsilon}{\partial x} + V\frac{\partial \alpha_l \varepsilon}{\partial y} + W\frac{\partial \alpha_l \varepsilon}{\partial z} = \frac{\partial}{\partial x}\left(\alpha_l \frac{\nu_t}{\sigma_\varepsilon}\frac{\partial \varepsilon}{\partial x}\right) + \frac{\partial}{\partial y}\left(\alpha_l \frac{\nu_t}{\sigma_\varepsilon}\frac{\partial \varepsilon}{\partial y}\right) + \frac{\partial}{\partial z}\left(\alpha_l \frac{\nu_t}{\sigma_\varepsilon}\frac{\partial \varepsilon}{\partial z}\right) - \frac{\alpha_l C_2 \varepsilon^2}{K} + \alpha_l \frac{C_1 \varepsilon \nu_t}{K}\left[2\left(\frac{\partial U}{\partial x}\right)^2 + 2\left(\frac{\partial V}{\partial y}\right)^2 + 2\left(\frac{\partial W}{\partial z}\right)^2 + \left(\frac{\partial U}{\partial y} + \frac{\partial V}{\partial x}\right)^2 + \left(\frac{\partial U}{\partial z} + \frac{\partial W}{\partial x}\right)^2 + \left(\frac{\partial V}{\partial z} + \frac{\partial W}{\partial y}\right)^2 \right] \quad \text{(Eq 15)}$$

where

$$\nu_e = \nu_m + \nu_t = \nu_m + \frac{C_3 K^2}{\varepsilon} \quad \text{(Eq 16)}$$

The values of the empirical constants are listed in Table 1.

2.2.4 Height Function Method for Monitoring Variation of Free Surface

In this study, a height function $H(x,z,t)$ is used to monitor the variation of the free surface after the velocity field has been calculated (Ref 7). The governing equation for the height function is:

$$\frac{\partial H}{\partial t} + U\frac{\partial H}{\partial x} + W\frac{\partial H}{\partial z} = V \quad \text{(Eq 17)}$$

2.2.5 Transport Equation for Species

To evaluate the mixing characteristics of the gas-stirred ladle, a mass transport equation must be used:

$$\frac{\partial \alpha_l C}{\partial t} + U\frac{\partial \alpha_l C}{\partial x} + V\frac{\partial \alpha_l C}{\partial y} + W\frac{\partial \alpha_l C}{\partial z} = \frac{\partial}{\partial x}\left[\alpha_l D_e \frac{\partial C}{\partial x}\right] + \frac{\partial}{\partial y}\left[\alpha_l D_e \frac{\partial C}{\partial y}\right] + \frac{\partial}{\partial z}\left[\alpha_l D_e \frac{\partial C}{\partial z}\right] \quad \text{(Eq 18)}$$

where the following relationship is assumed to exist:

$$\frac{D_e}{D} = \frac{\nu_e}{\nu} \quad \text{(Eq 19)}$$

The mixing efficiency is evaluated in terms of a "mixing time," which is defined as follows. When the gas stirring operation has reached the steady state, a known amount of tracer is injected from a certain position into the ladle in the time elapse of a pulse. The concentrations of the tracer are then measured at various locations of the ladle. As the tracer concentrations of all the measuring points have reached the equilibrium tracer concentration within 5%, the time between then and the tracer injection is defined as the mixing time. Naturally, shorter mixing time means better mixing.

2.2.6 Boundary Conditions

These boundary conditions are used in the model:

- At the side wall and bottom wall, normal velocity components vanish and no-slip boundary conditions are employed.
- On the free surface of the liquid, tangential stress is zero and normal stress equals applied pressure, and no fluxes cross the surface. This is expressed as:

$$\frac{\partial K}{\partial y} = \frac{\partial \varepsilon}{\partial y} = \frac{\partial \alpha_l}{\partial y} = \frac{\partial U}{\partial y} = \frac{\partial W}{\partial y} = 0 \quad \text{(Eq 20)}$$

3. Numerical Method

The flow equations described in the previous section are a set of nonlinear partial differential equations that are difficult to solve by analytical methods. Therefore, they must be solved by numerical methods.

In the present study, a computational fluid dynamics scheme called the SOLA (solution algorithm) method (Ref 8) was used to solve the flow equations. The system was first divided into a number of equal rectangular cells. The SOLA scheme, which was improved and extended from the MAC (maker and cell) technique, uses an explicit finite-difference method with pres-

Table 1 Values of the empirical constants of the *K*-ε model

Constant	Value
C_1	1.44
C_2	1.92
C_3	0.09
σ_k	1.00
σ_ε	1.30

sure p and velocity components U, V, and W as the primary dependent variables.

Numerical procedures were carried out to solve the time-dependent incompressible fluid flow equations and the turbulence equations simultaneously with the imposed wall and free surface boundary conditions using the height function method. As the steady-state velocity field is obtained, a prescribed amount of tracer is added to a prescribed location of the ladle. The tracer is then redistributed in the ladle based on Eq 18. Tracer concentrations in six different locations in the ladle are then monitored. The time for all six concentrations to reach within 0.95 to 1.05 of the equilibrium tracer concentration is defined as the mixing time. Figure 4 shows a set of typical concentration-time curves.

4. Results and Discussion

Based on the SOLA-SURF technique and the K-ε two-equation turbulence model, a 3-D mathematical model has been developed to analyze the fluid flow phenomena, including velocity field, bubble pathlines, surface fluctuation, and mixing condition, under various operating conditions for a ladle with and without an immersion hood. The ladle is 0.78 m in diameter and 0.96 m in height. The liquid level in the ladle was 0.7 m high. The ladle was first divided into a 21 by 12 by 21 (in the x, y, and z directions) mesh system. The increments in the x, y, and z directions were 0.041, 0.082, and 0.041 m, respectively. Flow patterns are displayed using velocity vectors in a 3-D isoparametric view as well as 2-D sectional view. The 2-D sectional views include vertical planes and horizontal planes. The vertical planes are cut through the porous plug parallel to the coordinate axes. The horizontal planes are perpendicular to the y-axis and include the top surface plane. In the present model, the bubbles were assumed to be released from the porous plug with constant frequency and with a certain bubble size distribution of 0.7 to 1.4 D_b, where D_b is the bubble size obtained from Eq 13.

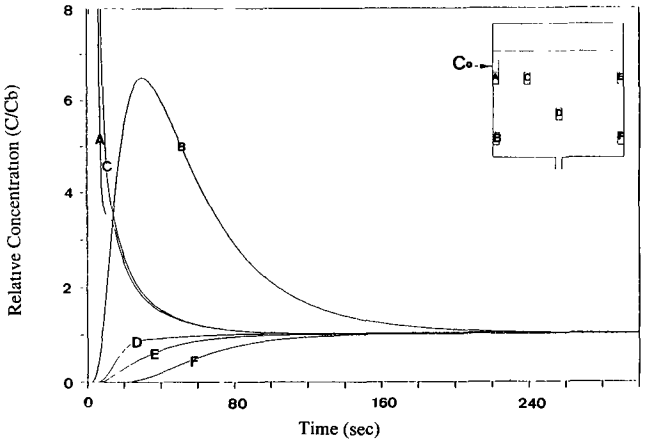

Fig. 4 Set of typical relative concentration-time curves to illustrate the mixing characteristics in a gas-stirred ladle

4.1 *Effects of Porous Plug Location on Flow Field*

Most industrial gas-stirred ladles have their porous plugs located off-center, which is believed to create a better stirring effect than when the porous plus is centered. Therefore, we need to understand the effects of porous plug location on the flow field in the gas-stirred ladle. In this study, three plug positions were investigated: at the center, one-third of the ladle diameter distance away from the ladle wall, and one-fourth of the ladle diameter distance away from the ladle wall.

The gas flow rate was fixed at 30 L/min. Figures 5(a) to (c) show the velocity fields in the gas-stirred ladles. From Fig. 5(a), it can be seen that the center-located porous plug case has recirculating flows in the upper portion of the ladle, while the bottom portion of the ladle remains rather inactive. The off-centered cases also form two recirculating flows in the upper portion of the ladle, as shown in Fig. 5(b) and (c). However, one of the recirculating flows is larger and stronger than the center

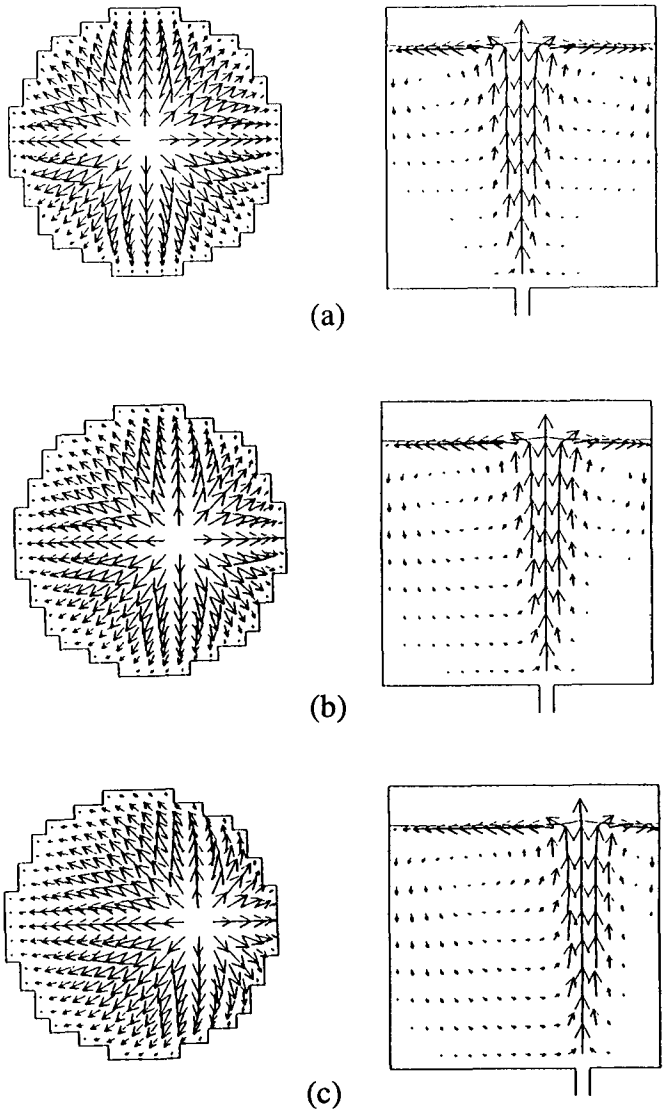

Fig. 5 2-D sectional views (horizontal and vertical) of the flow pattern for the gas-stirred ladle where the porous plug is located at one-half (a), one-third (b), and one-fourth (c) of the ladle diameter and the gas flow rate if 30 L/min

stirring. The bottom portion under the larger recirculating flow is more active than that under the smaller recirculating flow.

Figure 6 shows the relation between mixing time and stirring location. The ladle with the porous plug located at one-fourth of the ladle diameter distance has the shortest mixing time.

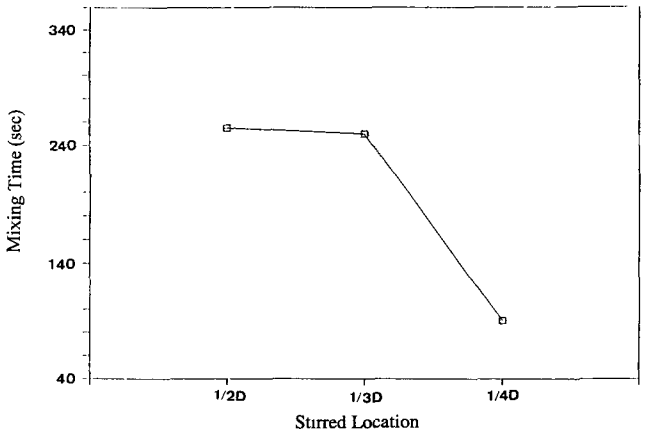

Fig. 6 Relation between mixing time and porous plug location

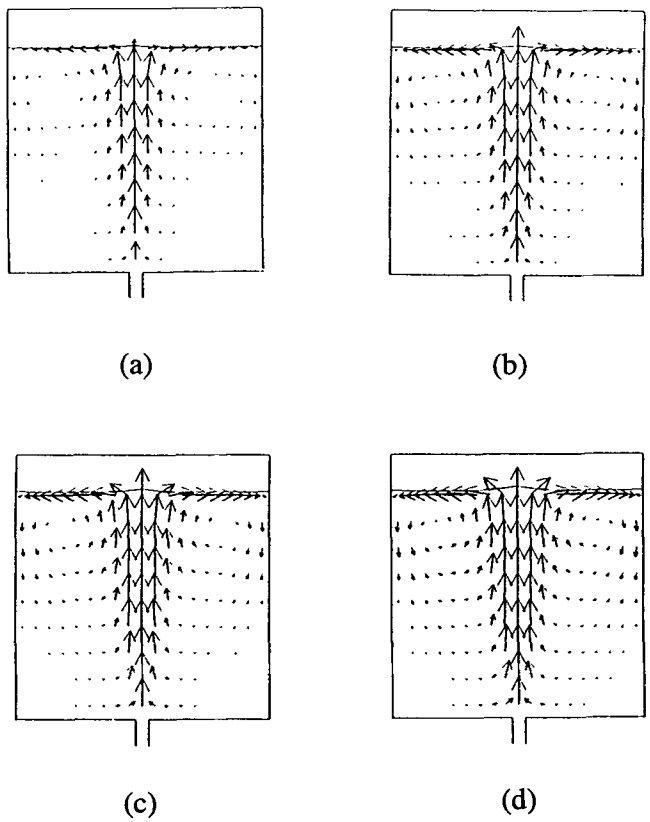

Fig. 7 2-D vertical sectional view of the flow pattern for the gas-stirred ladle where the porous plug is located at the center and gas flow rate is (a) 10, (b) 20, (c) 30, and (d) 40 L/min

4.2 *Effects of Gas Flow Rate on Flow Field*

Four gas flow rates (Q = 10, 20, 30, and 40 L/min) were used to study the effects of gas flow rate on the flow phenomena for centered stirring. The velocity fields for the gas-stirred ladle where the porous plug is located at the center are shown in Fig. 7(a) to (d). The flow patterns for the four gas flow rates are very similar. They all form recirculating flow in the upper portion and a fairly inactive zone in the bottom portion. Since bubble size and released frequency were increased with respect to gas flow rate, the drag force to drive the liquid to flow was also increased. This resulted in smaller inactive zones and higher surface velocities for higher gas flow rates

The relation between mixing time and flow rate is shown in Fig. 8. A linear relationship exists, where larger flow rate corresponds to shorter mixing time.

4.3 *Effects of Immersion Hood on Flow Field*

To evaluate the feasibility of the CAS process and to aid its design, the influence of the immersion hood as well as its size on the flow field was further investigated. Only the ladle with the centered plug was considered. Four hood diameters (0.37, 0.45, 0.53, and 0.62 m) were investigated under a gas flow rate of 30 L/min.

The influence of the immersion hood on the flow field depended on its size. The calculated flow patterns are shown in Fig. 9(a) to (d). Results showed that the fluid wave propagation along the free surface is stopped by the immersion hood and the liquid flows downward. Two recirculating vortices are formed and confined in the hood when the hood diameter is larger than 0.37 m. The free surface outside the immersion hood is rather quiet when the vortex is confined in the hood.

There is no apparent relationship between mixing time and hood size (Fig. 10). However, if the immersion hood is too small, the gas bubbles will float outside the hood and fluctuation cannot be confined inside the hood. To function properly in the CAS process, the immersion hood must be of the correct size.

4.4 *Multiplug Stirring*

In order to reduce the inactive zones in the bottom corner of the gas-stirred ladle, the feasibility of a multiplug has been ex-

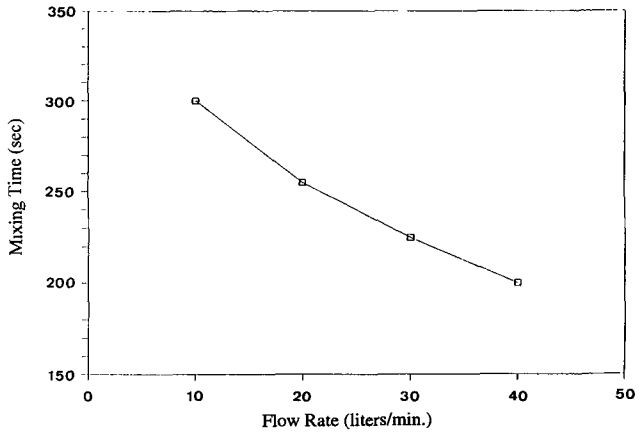

Fig. 8 Relation between mixing time and gas flow rates

amined. Three conditions were tested, all with a gas flow rate of 30 L/min. In the first case, there was only one porous plug, located at the center. In the second case, there were two porous plugs, 0.26 m apart from each other and 0.26 m away from the ladle wall. The gas flow rate from either plug was 15 L/min. In the third case, there were three porous plugs, arranged 120° apart in the circumferential direction and 0.246 m away from the ladle wall. The gas flow rate from each plug was 10 L/min. The computational results in Fig. 11 show that the flow patterns for the three cases are quite different. Where three plugs are used, the mixing time is shorter than the other cases (Fig. 12).

5. Conclusions

The mathematical model can be applied to study fluid flow phenomena in ladles stirred by argon gas. It provides detailed information that is difficult to obtain otherwise (e.g., velocity profiles).

In conventional gas-stirred ladles without an SAC operation, mixing is enhanced as the gas flow rate increases. However, the breakthrough zone also increases, owing to a larger plume zone and higher surface velocity.

The off-centered porous plug produces a different type of flow pattern in the ladle. The goals of various ladle metallurgy treatments can be achieved more effectively if flow patterns are properly controlled.

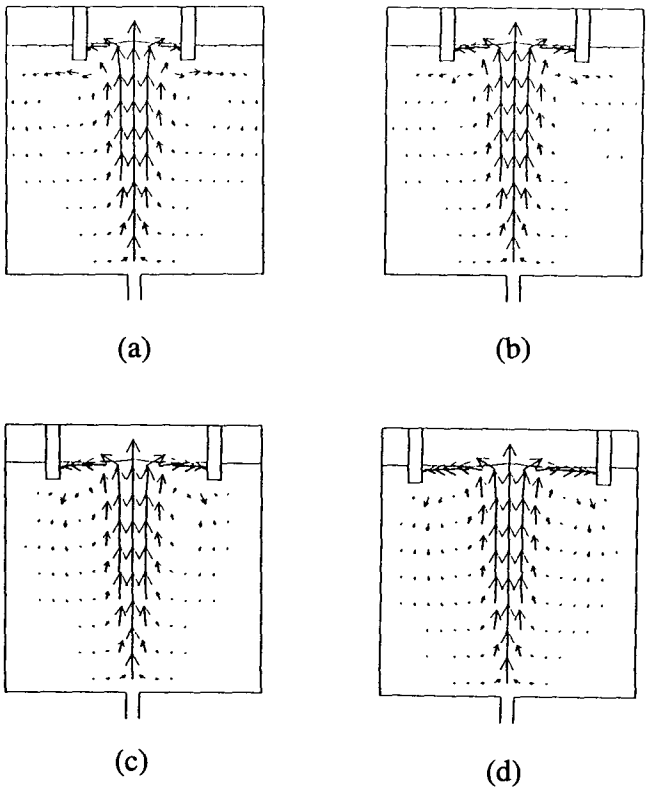

Fig. 9 2-D vertical sectional view of the flow pattern for the gas-stirred ladle where the porous plug is located at the center, the gas flow rate is 30 L/min, and the diameter of the immersion hood is (a) 0.37, (b) 0.45, (c) 0.53, and (d) 0.62 m

The SAC operation not only provides slag-free and good atmosphere control inside the hood, but also alters the flow patterns of the gas-stirred melt. The modified patterns tend to reduce the inactive zone in the bottom right corner and form a quiescent zone close to the free surface outside the hood. Subsequently, this can reduce slag entrapment and reoxidation.

With the SAC operation, the hood should be sufficiently large to confine the high-speed flow within the bubble plume. Otherwise, the melt and the bubbles will flow outward to the bulk liquid region and form a large recirculation, negating the advantages of the immersion hood. Therefore, an appropriately sized immersion hood must be chosen.

A three-plug operation significantly improves mixing compared to single-plug or two-plug operations.

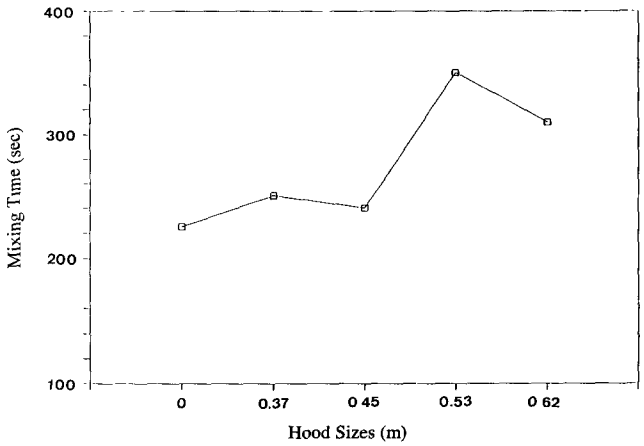

Fig. 10 Relation between mixing time and size of immersion hood

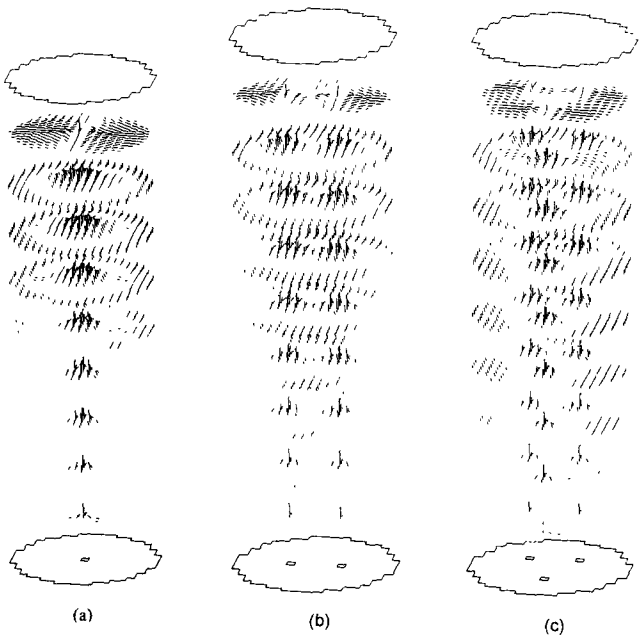

Fig. 11 3-D isoparametric view of the flow pattern for the gas-stirred ladle where the gas flow rate is 30 L/min and number of porous plugs is (a) one, (b) two, and (c) three

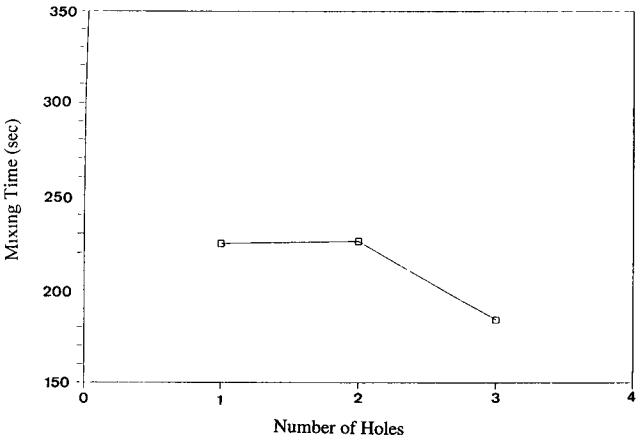

Fig. 12 Relation between mixing time and number of plugs

Acknowledgment

The authors thank the National Science Council of the Republic of China for sponsoring this research under contract no. NSC81-0405-E006-550.

References

1. L.E.K. Holappa, Review of Ladle Metallurgy, *Proc. SCANINJECT II Conf.*, MEFOS, 1980, p 1:1-1:23
2. Y.C. Lin and F.S. Shih, "The Water Model Study of Gas-Stirring Ladle in Slag and Atmosphere Control Process," Research report no. CSC-75-035, China Steel Corp., Kaohsiung, Taiwan, 1988
3. T. Harabuchi and K. Ohtsuka, *Proc. Symp. Steel Production Technology,* China Steel Corp., Kaohsiung, Taiwan, 1986, p 2A/8-1
4. J.D. Hwang, Y.C. Lin, and W.S. Hwang, Fluid Flow Modeling of Gas Stirred Ladles with Immersion Hood, *Mater. Sci. Technol.*, Vol 6, 1990, p 376-382
5. J.F. Davidson and B.O.G. Schüler, *Trans. Inst. Chem. Eng.*, Vol 38, 1960, p 144
6. B.E. Launder and D.B. Spalding, *Mathematical Modeling of Turbulence, Academic Press, London, 1972*
7. C.W. Hirt, B.D. Nichols, and N.C. Romero, "SOLA-SURF—Basic Solution Algorithm for Flows Bounded by Curved Surfaces," Report no. LA-5852 (Part 2), Los Alamos Scientific Laboratory, 1975
8. C.W. Hirt, B.D. Nichols, and N.C. Romero, "SOLA—A Numerical Solution Algorithm for Transient Fluid Flows," Report no. LA-5852 (Part 1), Los Alamos Scientific Laboratory, 1975